The EMBO Journal vol.13 no.9 pp.2066-2074, 1994

# Genetic analysis of cell morphogenesis in fission yeast—a role for casein kinase II in the establishment of polarized growth

**Valery Snell and Paul Nurse**

ICRF Cell Cycle Laboratory, Imperial Cancer Research Fund, PO Box 123, Lincoln's Inn Fields, London WC2A 3PX, UK

Communicated by P.Nurse

**We have initiated a study to identify genes regulating cell morphogenesis in the fission yeast *Schizosaccharomyces pombe*. Five genes have been identified, *orb1–orb5*, whose mutation gives rise to spherical cells, indicative of an inability to polarize growth. Two further genes have been identified, *tea1* and *ban1*, whose mutant alleles have disturbed patterns of tip growth, leading to T-shaped and curved cells. In fission yeast, sites of cell wall deposition are defined by actin localization, with actin distributions and therefore growth patterns undergoing cell cycle stage-specific reorganization. Studies of double mutants constructed between *orb5*-19 and various cdc mutants blocked before and after cell division show that *orb5* is required for the re-establishment of polar growth following cytokinesis. This indicates that the mutant allele *orb5*-19 is defective in the reinitiation of polarized growth, even though actin reorganization to the cell tips occurs normally. *orb5* encodes a fission yeast homologue of casein kinase II α. We propose that this kinase plays a role in the translation of cell polarity into polarized growth, but not in the establishment of polarity itself.**

*Key words*: actin/casein kinase II/fission yeast/growth polarity/morphology

## Introduction

The question of how a cell maintains a defined shape has long been of interest to biologists. An important aspect of this problem is the generation and maintenance of cell polarity. This phenomenon is widespread; for example, in the transmission of a nerve impulse, the uptake of nutrients by the microvilli of epithelial cells and the determination of the dorsal–ventral axis in embryonic development. Both cell growth and cell division can be polarized, with the latter playing an important role, particularly during early development where polar divisions can affect the fate of many cells in an organism (see Strome, 1993). The mechanisms generating cellular polarity are not understood, but are likely to involve cytoskeletal components and the proteins which interact with them. Genetic analyses in budding yeast have identified a number of genes involved in maintaining polarity during bud growth. These include *CDC24*, *CDC42*, *CDC43* and *BEM1*, which are essential for polarized growth, and the *BUD* genes which specify bud position. Altered budding patterns are also seen in cells carrying mutations in *SPA2*, *PFY1* or *CAP*. Many of these genes encode Ras-like products and their interacting control proteins [see Chant and Pringle (1991) and Madden *et al.* (1992) for reviews].

The cylindrical rod-shaped cells of the fission yeast *Schizosaccharomyces pombe* grow in length by tip extension (Streiblova and Wolf, 1972). The detailed pattern of growth depends on cell cycle stage; immediately after septation, daughter cells initiate elongation from the 'old' ends—the ends which existed in the previous cell cycle. On passing a point in $G_2$ termed 'New End Take Off' (NETO) (Mitchison and Nurse, 1985), growth continues from both cell tips in a bipolar fashion, until ~0.75 of a cell cycle has been completed. At this point, growth ceases and the cell enters a constant-volume stage prior to and during mitosis and cytokinesis. During this phase, tip growth ceases and is only re-established after cytokinesis when the 'old' ends begin growth again.

Areas of growth correlate with actin localization patterns visualized using phalloidin (Marks and Hyams, 1985) or by indirect immunofluorescence (Marks *et al.*, 1986). Just after septation, actin staining in the form of dots can be seen at the old end only. Bipolar staining is initiated at NETO and as cells enter the constant-volume stage, actin staining disappears from the cell tips and reappears as an equatorial filamentous ring, marking the position where the septum will form. Changes also occur in microtubule organization through the cell cycle; interphase cells possess an array of cytoplasmic microtubules extending between the cell tips (Marks *et al.*, 1986) which disappears at mitosis and is replaced by the mitotic spindle (Hagan and Hyams, 1988). After mitosis, spindle microtubules are depolymerized and the interphase array is re-established from two γ-tubulin-containing microtubule-organizing centres at the cell equator (Hagan and Hyams, 1988; Horio *et al.*, 1991). In fission yeast, cytoplasmic vesicles have been observed whose localization correlates with that of the actin dots (Kanbe *et al.*, 1989; Heath, 1990); these vesicles may be directed along cytoplasmic actin microfilaments to sites of wall synthesis. Treatment of reverting protoplasts with cytochalasin D disrupts actin localization, accompanied by inhibition of cell wall deposition, although it is not known whether actin controls this cell growth directly or indirectly (Kobori *et al.*, 1989). An inability to correctly organize cytoskeletal components directing cytoplasmic vesicles to sites of cell expansion, or a defect in vesicle transport, could result in depolarized growth.

Given its regular shape and highly polarized cell cycle-dependent mode of growth, fission yeast is an attractive system for use in the study of cell form, since abnormal patterns of growth are readily detectable from a simple visual screen. A variety of mutant fission yeast strains have been identified which display abnormal morphologies, and are summarized in Table I. *nda3* (Toda *et al.*, 1983; Umesono *et al.*, 1983b) encodes β-tubulin (Hiraoka *et al.*, 1984); a mutant in this gene produces some cells which are branched

**Table I.** Morphological mutants of *S.pombe*

| Gene | Phenotype | Gene product | References |
|---|---|---|---|
| *ras1Δ* | rounded; sterile | ras | 1, 2, 3 |
| *ral2* | rounded; sterile | ras activator? | 4 |
| *ral1,3,4* | rounded/'dumpy'; sterile | | 4 |
| *kin1 Δ* | rounded | protein kinase | 5 |
| *cwg1/pap1* | osmotically sensitive; rounded | | 6, 7 |
| *cwg2* | osmotically sensitive; rounded | *CDC43*-like | 7, 8 |
| *scd1Δ* | rounded; conjugation defect | *CDC24*-like | 9, 10 |
| *cdc42SpΔ* | rounded | *CDC42*-like | 11 |
| *pck2 Δ* | rounded/pear-shaped | protein kinase C | 12 |
| *ppe1 Δ* | rounded | protein phosphatase | 13 |
| *nda3* | mitotic arrest; branching | β-tubulin | 14, 15 |

Reference key: 1. Fukui and Kaziro, 1985; 2. Fukui *et al.*, 1986; 3. Nadin-Davis *et al.*, 1986; 4. Fukui *et al.*, 1988; 5. Levin and Bishop, 1990; 6. Ribas *et al.*, 1991a; 7. Ribas *et al.*, 1991b; 8. Diaz *et al.*, 1993; 9. E.C.Chang, personal communication; 10. Chant and Pringle, 1991; 11. Miller and Johnson, 1994; 12. Toda *et al.*, 1993; 13. Shimanuki *et al.*, 1993; 14. Umesono *et al.*, 1983b; 15. Toda *et al.*, 1983.

or bent, and have asymmetrically placed nuclei. Cells incubated with a high concentration of thiabendazole display a similar phenotype (Umesono *et al.*, 1983a). The mutation or disruption of a number of genes produces cells which are pear-shaped or rounded, including homologues of *Saccharomyces cerevisiae CDC42* (Fawell *et al.*, 1992; Miller and Johnson, 1994) and *CDC43* (Diaz *et al.*, 1993), together with homologues of protein kinase C (Toda *et al.*, 1993) and an interacting phosphatase, *ppe1* (Shimanuki *et al.*, 1993).

In order to initiate a comprehensive study of the gene functions responsible for organized polarized morphology in fission yeast, we carried out a visual screen for mutants whose growth had been altered to produce abnormally shaped cells. We have found mutants that generate branched and curved cells, but by far the commonest phenotype was rounded cells. We screened for mutants which were perfectly (or very nearly) spherical since we reasoned that cells whose polarity had been completely disrupted should exist as spheres. We describe the isolation of a number of spherical mutants which fall into five linkage groups: *orb1–orb5*. Our analysis has shown that one of these, *orb5*, is required for the re-establishment of polarized tip growth following cytokinesis, and that it encodes a fission yeast homologue of the casein kinase II α subunit.

## Results

### *Screen for morphological mutants*

We visually screened wild-type cells mutagenized with *N*-methyl-*N'*-nitro-*N*-nitrosoguanidine for clones displaying abnormal morphologies. After initial selection, mutants were incubated at 25°C until small colonies formed, then replica plated to 35.5°C. The penetrance of phenotypes was assessed by DAPI staining and counting the frequency of cells with abnormal morphologies. Eighteen mutant strains were selected which displayed a high frequency of cells with clearly abnormal morphology (Table II). Three major phenotypes were observed: spherical cells, 'T'-shaped cells and banana-shaped cells.

The phenotype identified most frequently was spherical cells. Mutants previously isolated which have similar phenotypes (Table I) tend to be pear-shaped rather than completely spherical. We screened specifically for mutants which were perfectly (or very nearly) spherical, reasoning that these mutants might be completely defective in polarized growth. Sixteen mutants fall into this class; 11 of these are temperature sensitive for sphere-forming ability, whilst the remaining five are spheres at all temperatures (Table II). The majority of spherical cells are uninucleate, with abnormal nuclear position (Figure 1). Instead of being equatorially placed, as is the case for rod-shaped wild-type cells, nuclear position was frequently off centre. This suggests that in

**Table II.** Phenotypes and linkage assignments of morphological mutants obtained by visual screen. Pairwise crosses and random spore analysis were used to place mutants into linkage groups

| Phenotype at 36°C | Gene | No. of alleles |
|---|---|---|
| Spherical—fertile | *orb 1* | 3 |
| | *orb2* | 4 |
| | *orb3* | 1 |
| | *orb4* | 1 |
| | *orb5* | 2 |
| Spherical—sterile | *ral1*? | 5 |
| 'T'-shaped | *tea1* | 2 |
| Bananas | *ban1* | 1 |

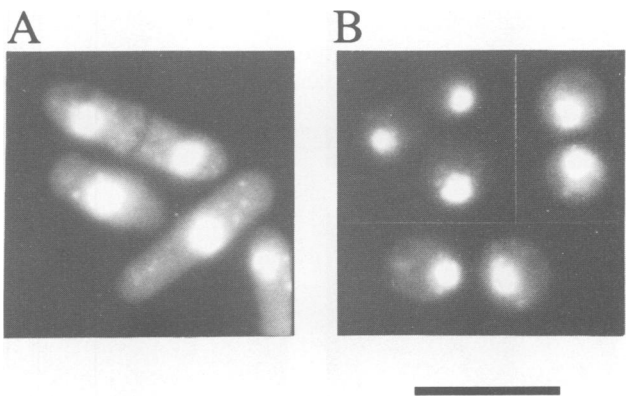


**Fig. 1.** Phenotype of spherical mutants by DAPI staining. (**A**) Wild-type strain *ade6*-M210 *leu1*-32 *h*⁻. (**B**) *orb5*-19. Cells were incubated at 35.5°C for 8 h and then stained with DAPI to reveal nuclear position. Note the spherical appearance of *orb5*-19 and the asymmetric nuclear position compared with wild type. Bar = 10 μm.

addition to their failure to grow in a polarized fashion, these cells cannot generate the normal positional signals which locate the nucleus centrally. The position of the nucleus and other organelles has been proposed to be controlled by cytoplasmic microtubules in fission yeast, given the unfixed nuclear position observed in *nda3* (see above) and the fact that the mitotic nuclei in *cdc25*-22 leaking past a block at the restrictive temperature wander from the cell centre when cytoplasmic microtubules disappear (Hagan and Hyams, 1988).

One mutant was obtained which formed a proportion of 'T'-shaped and bent cells at the restrictive temperature (Figure 2A). A second mutant having a similar phenotype was isolated in a separate mutagenesis (A.Woollard, personal communication). The strains are viable at 35.5°C and belong to the same linkage group, called *tea1* for *t*ip *e*longation *a*berrant. Time-lapse studies of *tea1*-1 at 35.5°C clearly show elongation occurring at the tip of the branch (Figure 2B). The cell on the left displays the 'T' phenotype; septation releases a cell with wild-type morphology. The cell on the right generates the 'bent' phenotype, with growth continuing from one end in a direction deviating from the normal orthogonal pattern of tip growth. DAPI staining of *tea1*-1 at 35.5°C reveals that cells are uninucleate. These cells appear to be unable to recognize the cell tips as growth zones, instead activating growth at an inappropriate position.

The third class of mutants, represented by one strain which has been named *ban1*, produces curved, banana-shaped cells similar to the bent cells seen in *tea1*. Both tea and ban mutants will be discussed further elsewhere.

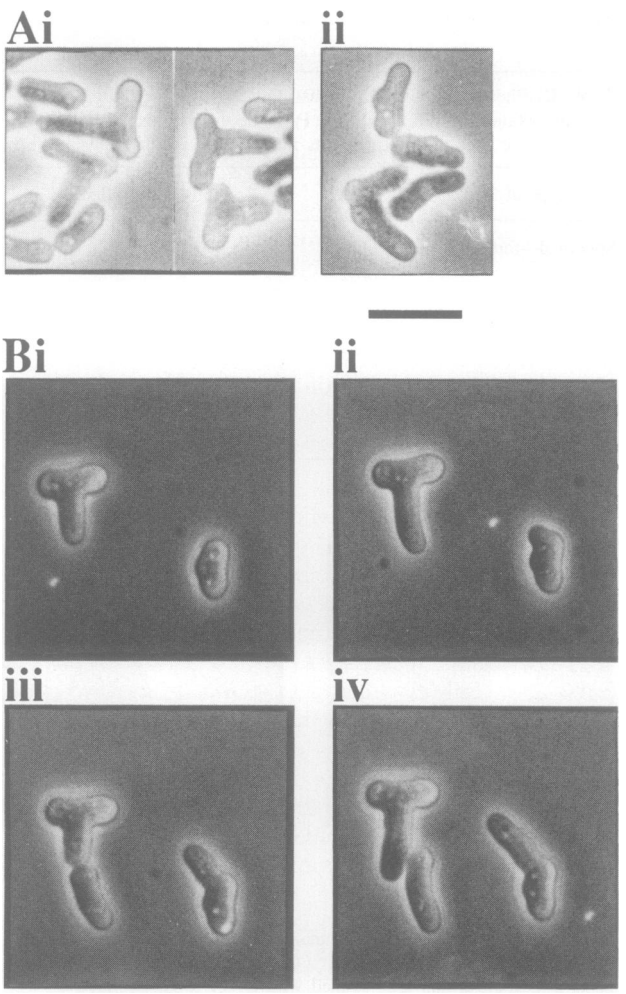


**Fig. 2.** Phenotypes of *tea1*-1. (**A**) Cells of *tea1*-1 growing at 35.5°C for 3 h on YEA and observed using phase-contrast microscopy. Populations showing the presence of 'T'-shaped (i) and 'bent' (ii) cells. These cells represent 70% of the population at this time point with the remainder appearing normal (see B). Also note the presence of cells possessing lateral bulges which may develop into branches. (**B**) Time-lapse study of *tea1*-1 growing at 35.5°C; photographs were taken at hourly intervals. Note that elongation appears to be continuing primarily from one tip. The development of both T-shaped and bent cells is seen; the cell on the left displays the 'T' phenotype, elongating from the tip of the branch and septating to release a daughter cell with apparently wild-type morphology (iii and iv). The cell on the right represents the 'bent' phenotype—growth continues from the tip in a direction deviating from the normal orthogonal pattern. Bar = 10 μm.

### *Genetic analysis of spherical mutants*

The 16 spherical mutants were back-crossed to a wild-type strain. The five non-conditional mutants were sterile (see later), whilst the remaining 11 showed 2:2 segregation of the temperature-sensitive phenotype both in random spore and tetrad analysis; thus, the phenotype is caused by a single chromosomal mutation in all cases. Phenotypes of $orb^{+}/orb^{-}$ diploids showed that all the mutations are recessive. Linkage analysis demonstrated that the mutants define five genes, *orb1*−*orb5*. The number of alleles of each gene suggests that this screen has not been saturated (Table II), although the fact that only five genes were defined by these 11 mutations make it unlikely that there will be a very large number of genes that can be mutated to this phenotype.

Mutations in a number of genes have been reported to produce rounded cells (Table I), although these generally tend not to be as spherical as orb cells. In order to determine whether the orb mutants carry mutations in any of these genes, representatives of *orb1*−*orb5* were either crossed to the mutant strains or transformed with multicopy plasmids carrying the gene of interest. None of the orbs was allelic with or rescued by any of the following genes: *cwg1*, *cwg2*, *kin1*, *ras1*, *ral1*, *ral2*, *ppe1*, *pck1* and *pck2*, although a partial effect of *pck1* on *orb4* was seen subsequently. *orb4* was shown to be allelic with *sts5*, which is also partially rescued by *pck1* (T.Toda, personal communication).

*ral* mutants and strains carrying a *ras1* deletion are rounded and sterile, and thus are similar to the sterile round mutants isolated in this study. We transformed the five sterile mutants with multicopy wild-type *ras1*, *ral1* and *ral2*, and looked for plasmid-linked rescue of the spherical phenotype. The shape defect of all five mutants was rescued by pDB248'*ral1* at both 25 and 35.5°C, but not by *ras1* or *ral2*. The rescue of sterility by multicopy *ral1* allowed us to use the five strains in crosses to show that each carries a single chromosomal mutation and that all five are allelic. These mutants carry mutations either in *ral1* itself or in gene whose product interacts with it.

### *Phenotype of orb5-19*

Alleles of *orb1*, *orb2* and *orb4* can form colonies on YEA at 35.5°C, and cell number continues to increase in cultures incubated at this temperature. The mutant of *orb3* survives the shift to 35.5°C less well, whilst *orb5*-19 is lethal at this temperature and so cannot form colonies on solid medium.

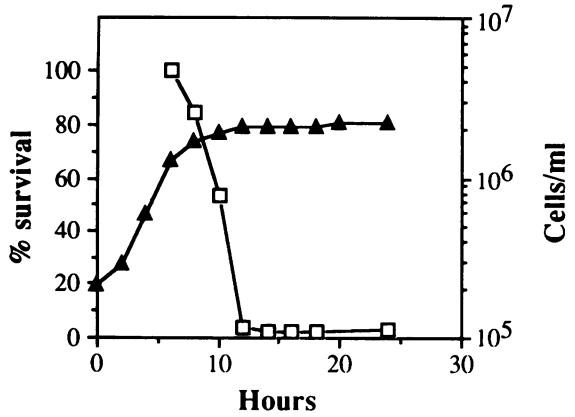


**Fig. 3.** Viability of *orb5*-19 at 35.5°C. *orb5*-19 was cultured at 25°C and shifted to 35.5°C at time 0. The graph shows cell number increase (▲) and viability (□), determined as described in Materials and methods.

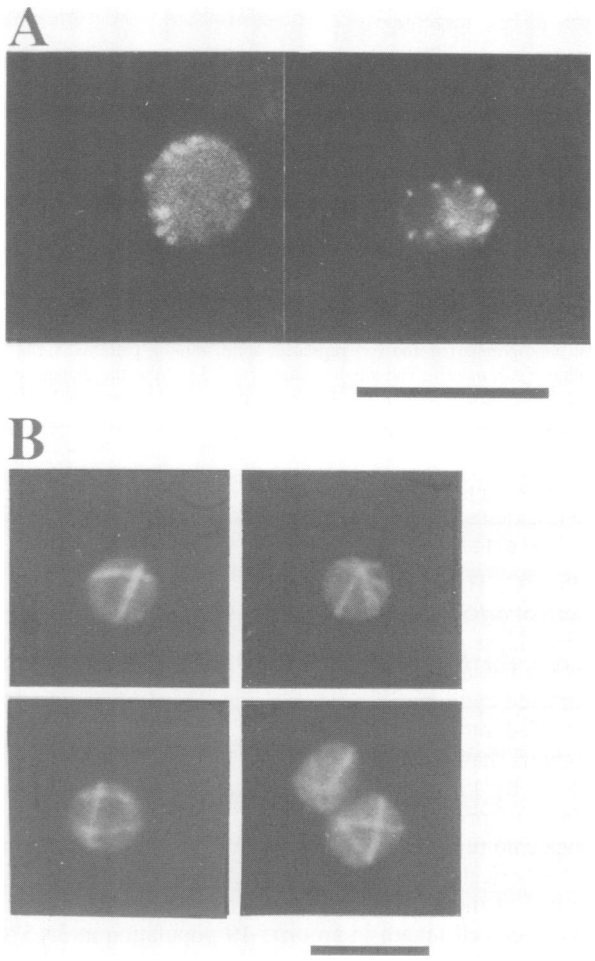


**Fig. 4.** The cytoskeleton of *orb5*-19 is less ordered than that of wild-type cells. Indirect immunofluorescence of *orb5*-19 incubated at the restrictive temperature. (**A**) Actin distributions in *orb5*-19. Note that actin is apparently distributed throughout the cell. (**B**) Interphase microtubule distributions in *orb5*-19. Microtubules appear to form a criss-cross pattern rather than the wild-type 'end-to-end' pattern. Bars = 10 μm.

It goes through 2−3 cell divisions at this temperature before arresting as small round cells (Figure 3).

We focused on *orb5*-19 because it is lethal at the restrictive temperature and is a recessive mutation, suggesting that *orb5*

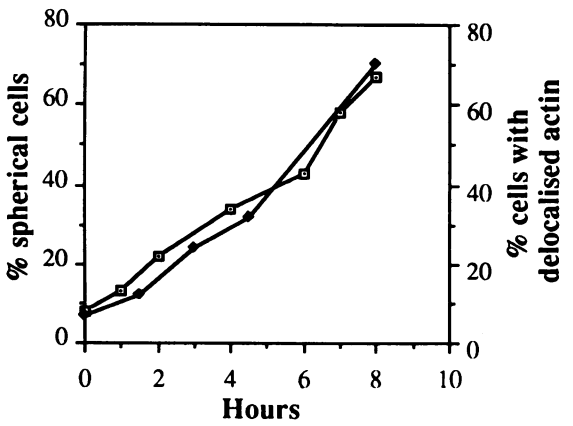


**Fig. 5.** Development of the *orb5*-19 phenotype. The frequencies of spherical cells (□) and cells with delocalized actin (♦) on incubation at 35.5°C are shown.

may be essential for viability. Both tubulin and actin patterns assessed using immunofluorescence in *orb5*-19 were disturbed compared with wild type: microtubules criss-crossed the spherical cells (Figure 4B), whilst actin dots were distributed in an apparently random fashion (Figure 4A). When *orb5*-19 is incubated at 35.5°C, the phenotype develops from 'wild-type', rod-shaped cells, through short cells whose actin and microtubule distributions resemble those of wild-type cells, to the terminal phenotype of spherical cells with the apparently abnormal cytoskeletal distributions described above. The appearance of cells possessing 'delocalized' actin staining patterns parallels the appearance of spherical cells in the population (Figure 5). An identical phenotype was observed in diploids homozygous for *orb5*-19.

### *orb5 plays a role after cell division*

The fact that several rounds of division are required at the restrictive temperature before *orb5*-19 becomes fully spherical suggests that progression through the cell cycle may be required to generate the mutant phenotype, in particular the relocalization of growth to the old ends of the daughter cells after cell division. The defect in *orb5*-19 could potentially result from an inability to re-initiate tip elongation after mitosis. In order to evaluate this possibility, we constructed double mutants between *orb5*-19 and various temperature-sensitive cell division cycle (cdc) mutants: *cdc10*-129, which blocks in $G_1$; *cdc25*-22, which blocks in $G_2$; *cdc2*-33, which blocks mainly in $G_2$; and *cdc11*-119, a septation mutant which undergoes repeated nuclear divisions and actin relocalizations, without intervening septation. These mutants possess actin distributions characteristic of the position in the cell cycle at which they block. *cdc2*-33 and *cdc25*-22 do not undergo the growth transitions associated with mitosis, cytokinesis and the re-establishment of polarized growth, whilst *cdc10*-129 and *cdc11*-119 do (Marks *et al.*, 1986). Double mutants with *cdc2*-33 and *cdc25*-22 arrest before mitosis, and thus before the new-to-old end growth- and actin-transition; therefore, if our view is correct, double mutants should display the cdc phenotype. However, *orb5*-19 *cdc10*-129 goes through a single mitosis before arresting in $G_1$ of the following cell cycle. If actin is not relocalized in these cells, or if tip elongation is not reinitiated, we would expect them to be unable to elongate. Similarly, cells of *orb5*-19 *cdc11*-119

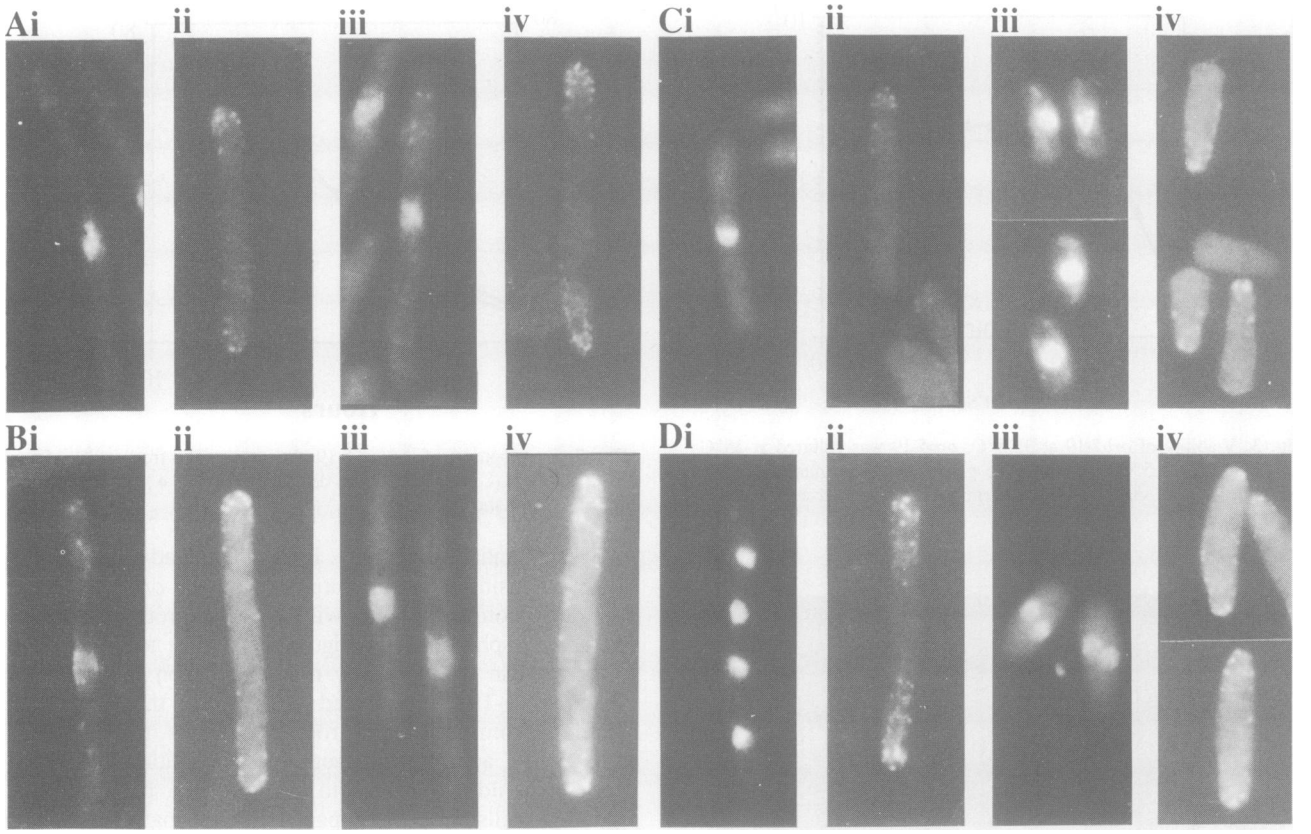


**Fig. 6.** *orb5* is required for the re-establishment of polarized growth after cell division. Phenotypes of double mutants between *orb5*-19 and various cdc mutants. For (**A–D**), photographs (i) and (iii) represent DAPI staining, whilst photographs (ii) and (iv) represent actin staining patterns. Cells were cultured at 25°C, then shifted to 35.5°C for 3.5 h prior to fixation and staining. (Ai) and (ii) The single mutant *cdc2*-33. Note the elongated cdc$^-$ phenotype, single nucleus and bipolar actin staining. (iii) and (iv) The double mutant *orb5*-19 *cdc2*-33. The phenotype is indistinguishable from that of the *cdc2*-33 single mutant. (Bi) and (ii) *cdc25*-22; (iii) and (iv) *orb5*-19 *cdc25*-22. The phenotypes of both single and double mutants are like those in (A). (Ci) and (ii) *cdc10*-129. Cells are elongated with unipolar actin staining. (iii) and (iv) *orb5*-19 *cdc10*-129. Elongation has not taken place, but actin relocalization clearly has. (Di) and (ii) *cdc11*-119. This is an early septation mutant which undergoes repeated rounds of mitosis, including the actin relocalizations associated with cell division; the majority of cells display a bipolar actin staining pattern. (iii) and (iv) *orb5*-19 *cdc11*-119. The double mutant becomes multinucleate at the restrictive temperature (binucleates are shown here, although cells with four nuclei are also seen) and displays a bipolar actin staining pattern, although cells cannot re-establish elongation after actin relocalization.

would go through repeated nuclear division cycles, but would be unable to elongate during the intervening periods.

When the double mutants were incubated at 35.5°C for 3.5 h, the phenotypes were consistent with the view that *orb5* is required for the re-establishment of polarized tip growth following the constant-volume phase of mitosis: *orb5*-19 *cdc2*-33 and *orb5*-19 *cdc25*-22 were elongated and uninucleate, *orb5*-19 *cdc10*-129 was short and uninucleate, and *orb5*-19 *cdc11*-119 was short and multinucleate (Figure 6). Anti-actin immunofluorescence of these mutants revealed that cells blocked before mitosis (i.e. the *cdc2*-33 and *cdc25*-22 double mutants) had the anticipated bipolar actin staining patterns characteristic of the single cdc mutants. The double mutants with both *cdc10*-129 and *cdc11*-119 also had the same actin staining patterns as the single mutants, and thus must have undergone actin relocalization successfully, even though they fail to elongate at these poles (Figure 6). *orb5* is therefore not required for establishment of actin localization or cell polarity after mitosis, but is involved in translating these factors into polarized growth.

### *orb5-19 is defective in cell elongation*

If *orb5*-19 cannot translate actin polarization into cell tip elongation after cell division, then the ability of a cell population to elongate should gradually diminish after a shift to 35.5°C. This was evaluated by following the elongation pattern of *orb5*-19 cells growing at the restrictive temperature by time-lapse photography. Figure 7Ai shows a cell at time 0 which has already septated and, although it has not yet completed cytokinesis, the two daughter cells have already proceeded into the next cell cycle. Two hours later, the two daughters have elongated during the first cell cycle at 35.5°C. By 4 h at the higher temperature, the two cells have divided to produce four daughter cells. These cells can elongate no further before cell division and thus produce the eight spherical or nearly spherical cells seen in Figure 7Aiv. The cell at the top of the group has died.

Average cell length in an *orb5*-19 population at 35.5°C decreases with continued incubation at this temperature without a significant alteration in width, and the length:width ratio in these cells tends to 1, as would be expected for spherical cells; the ratio decreases from 3.12 to 1.37 over a 10 h incubation at 35.5°C. By combining the data for cell number increase with average cell length in this culture, we obtain a view of the extent of cell elongation in the overall culture. If this is compared with similar data for a wild-type culture growing at 35.5°C, we clearly see that cell elongation is gradually reduced in *orb5*-19 as cells undergo divisions at 35.5°C, in agreement with the hypothesis proposed above (Figure 7B). This also accounts for the drop in cell viability.

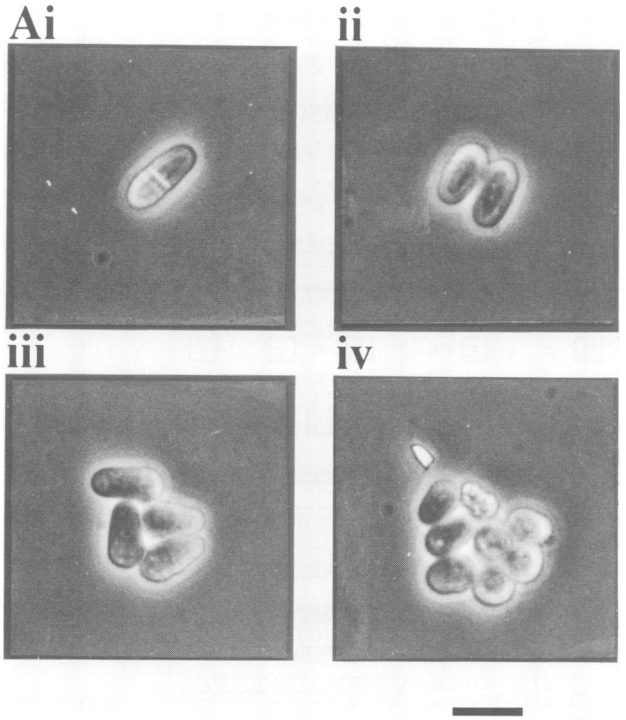


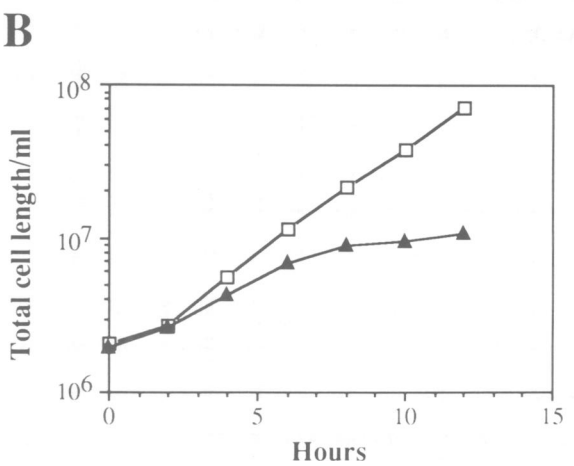


**Fig. 7.** *orb5*-19 is defective in re-establishing cell elongation after cell division. (**A**) Time-lapse studies of *orb5*-19 at 35.5°C. Cells were observed using phase-contrast microscopy and photographed at 2 hourly intervals. (i) Time = 0 h. (ii) Time = 2 h. (iii) Time = 4 h. (iv) Time = 6 h. See the text for details. Bar = 10 μm.
(**B**) Comparison of the rate of total cell elongation within a culture of *orb5*-19 incubated at 35.5°C. Wild-type cells (□) continue to divide and elongate at the higher temperature, but after an initial increase (probably due to cells which had already established polarized growth at the time of the shift up) total elongation in the *orb5*-19 culture ceased (▲). Cells were cultured at 25°C and then shifted to 35.5°C at time 0.

### *Cloning the orb5 cDNA*

We cloned *orb5* cDNA by complementation of the temperature-sensitive lethal phenotype using a library of *S.pombe* cDNAs (Kelly *et al.*, 1993). Three plasmids were isolated which rescued lethality, cell shape and nuclear position in *orb5*-19 at 35.5°C (Figure 8), and were shown to be related by both Southern and sequencing analysis. A 1.5 kb cDNA insert under the control of the *nmt1* promoter was subcloned into a vector carrying both *LEU2* and *sup3*-5, a nonsense suppressor of the *ade6*-704 mutation. We

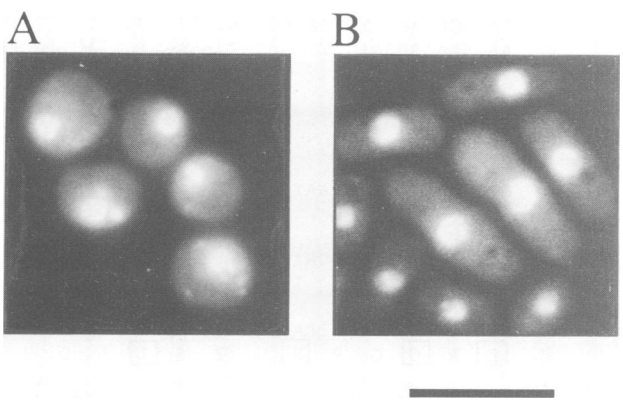


**Fig. 8.** Rescue of *orb5*-19 by pREP3X-*orb5*. Cells were incubated at 35.5°C for 8 h, then DAPI stained. (**A**) *orb5*-19. (**B**) *orb5*-19 transformed with pREP3X *orb5* at 35.5°C. Note the rescue of shape and nuclear position. Small cells have probably lost the plasmid and are nutritionally starved. Bar = 10 μm.

transformed this construct into *orb5*-19 *leu1*-32 *ade6*-704 and selected stable adenine prototrophs. In a cross between one of these isolates and *ade6*-704 *leu1*-32, no recombinants were seen out of 3411 spores; and in a cross with *orb5*-19 *ade6*-704 *leu1*-32, rescue of lethality was tightly linked with adenine prototrophy. Thus, the *LEU2*, *sup3*-5 and *orb5* markers had integrated within 0.5 cM of the *orb5* gene, and the cDNA is derived from the *orb5* gene rather than a suppressor.

The 1.5 kb *orb5* cDNA was sequenced on both strands and upstream sequences were obtained from the larger cDNAs using dideoxy chain termination reactions. The sequence contains a single open reading frame (ORF) potentially encoding a peptide of 332 amino acids (Figure 9). The predicted peptide sequence was compared with sequences in the SwissProt database and shows a high degree of identity with the α and α′ subunits of casein kinase II from a variety of species. The residues Thr112 and Pro113 correspond to the motif phosphorylated by proline-dependent protein kinase identified in higher eukaryotes (Hall and Vulliet, 1991), but the relevance of this for the *orb5*-encoded casein kinase II remains unknown.

Kinase activity towards casein was examined in extracts of wild type (*972h*$^-$) and *orb5*-19 cultured to exponential growth and harvested either at 25°C or after an 8 h incubation at 37°C. Using the reaction conditions described in Materials and methods, we assessed the level of casein kinase activity in each extract by the amount of incorporation of radioactive label into casein. The following scintillation counting data were obtained: 736 c.p.m. for wild type harvested at 25°C; 597 c.p.m. for wild type harvested at 37°C; 637 c.p.m. for *orb5*-19 harvested at 25°C; 139 c.p.m. for *orb5*-19 harvested at 37°C. Thus, casein kinase activity is reduced to 23% of wild-type levels in an extract from the mutant after a shift to the restrictive temperature, consistent with the *orb5*-19 mutant being defective in casein kinase activity.

## Discussion

We have isolated fission yeast mutants that display abnormal morphologies and identified three major morphological phenotypes—spherical cells, branched cells (*tea1*-1 and

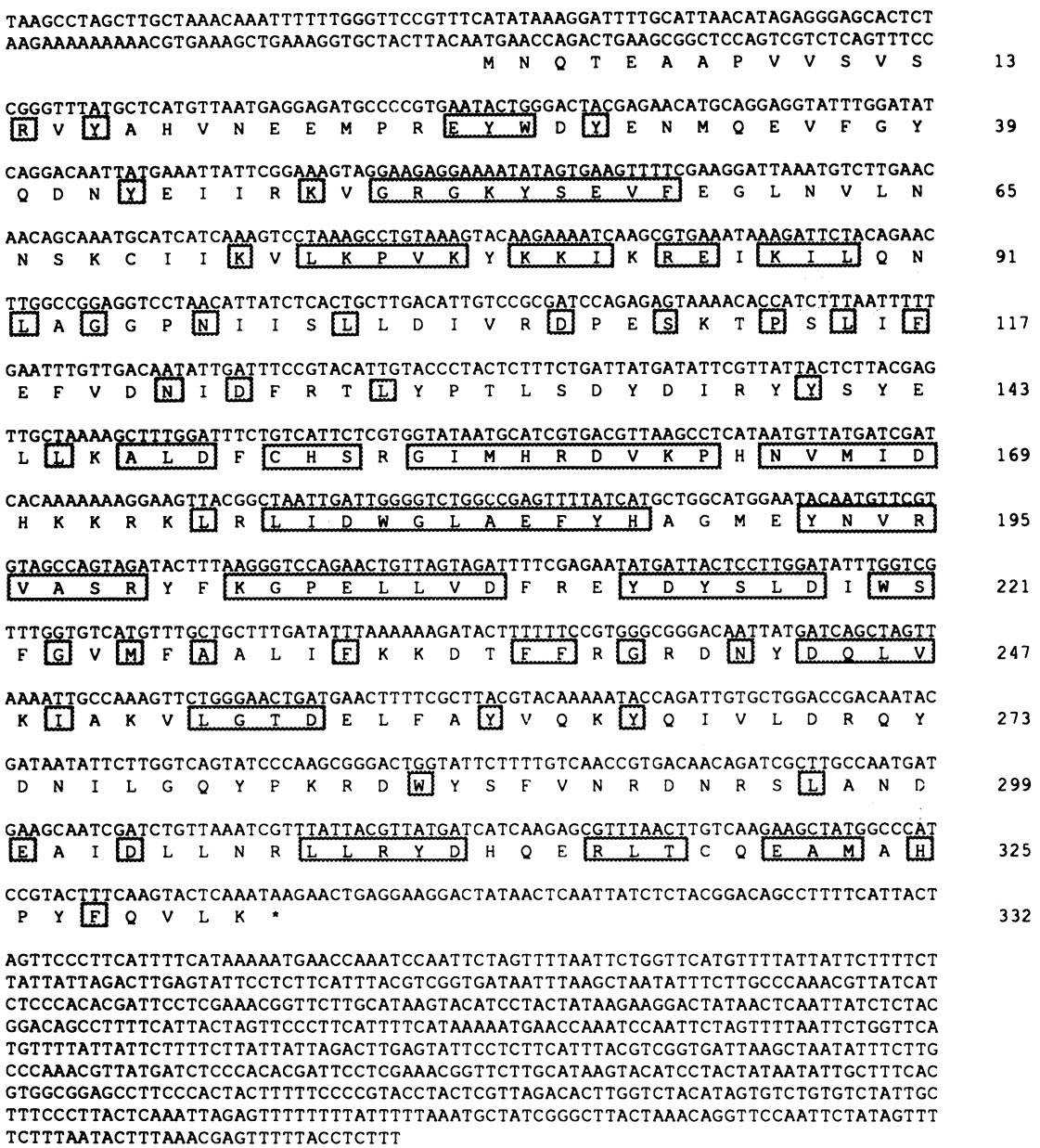


**Fig. 9.** Nucleotide and predicted peptide sequence of *orb5*. Sequence of the 1827 nucleotides comprising the ORF and flanking sequences, and of the 332 amino acids of the deduced sequence. The 3′ termination codon is indicated by an asterisk (*). Amino acid residues conserved between all CKII catalytic subunits isolated so far are boxed.

*tea1*-2) and curved cells (*ban1*)—with the first class being the most frequently observed. Mutations in at least five *orb* genes produce this phenotype; one of these, *orb5*, has been cloned and shown to encode a fission yeast homologue of casein kinase IIα. *orb5*-19 is specifically defective in the re-establishment of polarized growth after mitosis when actin is relocalized normally. Thus the spherical 'loss of polarity' phenotype can arise in two ways: first, from an inability to maintain polarity or to re-establish it after mitosis, and second from an inability to translate cellular polarity into polarized growth.

Mutants in *tea1* initiate growth from inappropriate positions, resulting in cells which are 'T'-shaped or angular. A low frequency of such cells is generated by cold-sensitive mutants in *nda3* (Toda *et al.*, 1983; Umesono *et al.*, 1983b) held for prolonged periods at the restrictive temperature, or cells treated with high concentrations of thiabendazole (Umesono *et al.*, 1983b), implicating disturbance to microtubule polarity in this phenotype. Some *tea1*-1 cells are bent, similar to the curved cells seen in *ban1*-1. *tea1*-1 can elongate and form colonies at the restrictive temperature, suggesting that an alteration in polarity is not necessarily lethal. The signal which marks cell tips as potential growing points in fission yeast is unknown; perhaps, a genetic hierarchy analogous to that in budding yeast also exists in fission yeast. Like *tea1* mutants, *bud* mutants are not lethal and do not affect cell growth other than to alter the site selected for budding (Chant and Herskowitz, 1991; Chant *et al.*, 1991).

The spherical cell phenotype of *orb5*-19 is generated over two rounds of division at 35.5°C, implicating cell cycle progression as being necessary for its establishment. In order

to investigate this, we constructed double-mutant strains between *orb5*-19 and a variety of cell division cycle (cdc) mutants which arrest at specific positions in the cell cycle (Nurse *et al.*, 1976)—see Results for details. The normal elongation in *orb5*-19 *cdc2*-33 and *orb5*-19 *cdc25*-22 mutants which become blocked in $G_2$ demonstrates that *orb5* is not necessary for polarized growth under these circumstances, and that the mechanism of cell wall biosynthesis is not itself disturbed. Rather, *orb5* is required for the re-initiation of polarized growth after mitosis, at the transition from the constant-volume stage at mitosis back to unipolar growth at the old end. This is consistent with the failure to elongate seen in *orb5*-19 *cdc10*-129 and *orb5*-19 *cdc11*-119, both of which undergo at least one mitosis at the restrictive temperature. In addition, since actin in these double mutants is properly localized at the cell tip(s), but growth does not occur, *orb5* is not involved in the establishment of actin localization or polarity, but rather in translating these factors into polarized growth. The terminal phenotype of the *orb5*-19 single mutant is delocalized actin distribution. The difference between this result and the clear actin polarization seen in the elongated double-mutant cells is because the single-mutant cells are of small size, making it impossible to distinguish polarized and depolarized distributions. The fact that the 'delocalized' distribution is only observed in the small spherical cells, and not in the shorter, cylindrical cells produced after the first cell division, is consistent with this view.

The data suggest that once actin has relocalized to the cell equator, the signals directing cell surface expansion to the cell tips in response to cytoskeletal organization are lost and cannot be re-established after cytokinesis. This is supported both by time-lapse studies and by measurements of total cell length in a growing population of cells, which show that the ability to elongate is diminished in a population growing at 35.5°C.

The phenotype of *orb5*-19 is in some ways similar to the effect of staurosporine (Toda *et al.*, 1991), an alkaloid inhibitor of protein kinases, particularly protein kinase C. It arrests fission yeast cells at a stage immediately following cell division and prevents their entry into the cell elongation stage after cytokinesis. This differs from the situation in *orb5*-19 in that cells treated with staurosporine do not continue through the cell cycle to undergo further division and thus presumably the target which is affected by the drug is essential for cell cycle progression as well as for cell elongation.

*orb5* has been cloned by complementation with a cDNA library. It encodes a fission yeast homologue of the catalytic subunit of casein kinase II (CKII), showing >70% sequence similarity with the gene cloned from organisms including *S.cerevisiae* (Chen-Wu *et al.*, 1988; Padmanabha *et al.*, 1990), *Drosophila melanogaster* (Saxena *et al.*, 1987), human (Meisner *et al.*, 1989; Lozeman *et al.*, 1990), chicken (Maridor *et al.*, 1991), *Dictyostelium discoideum* (Kikkawa *et al.*, 1992), *Caenorhabditis elegans* (Hu and Rubin, 1990) and *Zea mays* (Dobrowalska *et al.*, 1991). CKII is a serine/threonine protein kinase which has the subunit structure $\alpha 2\beta 2$ or $\alpha\alpha'\beta 2$ . Many substrates have been proposed based on the presence of consensus target sites for CKII or on *in vitro* studies (reviewed by Pinna, 1990), including a variety of proteins involved in gene expression or protein synthesis, and components of signalling pathways. Fission yeast casein kinase II $\alpha$ and $\beta$ subunits have recently been independently identified (Roussou and Draetta, 1994).

The CKII encoded by *orb5* clearly plays a role in the initiation of polarized growth. In fission yeast, this is thought to involve the delivery of cytoplasmic vesicles to the growing points of the cell at the sites of cortical actin dots. Cells with microtubular structures disrupted by mutation or chemical means have morphological abnormalities (Walker, 1982; Umesono *et al.*, 1983a,b) and *orb5*-19, which also has an abnormal microtubule array, cannot establish polarized growth. This contrasts with the situation in budding yeast, where microtubules do not seem to be involved in vesicle transport (Huffaker *et al.*, 1988; Jacobs *et al.*, 1988); polarized vesicle transport may occur parallel to actin filaments (reviewed by Heath, 1990), possibly via an actin−myosin-based system (Johnston *et al.*, 1991). In light of our demonstration of CKII involvement in polarized growth, studies on microtubules and CKII in neuroblastoma cells may be relevant. *In vitro* studies have shown that $\beta$-tubulin and MAP-1B are phosphorylated by CKII (Serrano *et al.*, 1987; Diaz-Nido *et al.*, 1988; Serrano *et al.*, 1989). Further, microinjection of an antisense CKII$\alpha$ oligodeoxyribonucleotide inhibits polarized neuritogenesis in neuroblastoma cells (Ulloa *et al.*, 1993), accompanied by site-specific dephosphorylation of MAP-1B at CKII target sites. From these and our own studies, we propose that casein kinase II$\alpha$ plays an important and possibly general role in the translation of polarity into polarized growth, perhaps by phosphorylating an as yet unidentified MAP-like protein influencing microtubular function.

## Materials and methods

### *Strains, media and plasmids*

All *S.pombe* strains used are isogenic to the wild type 972$h^-$. Standard genetic methods were as described (Moreno *et al.*, 1991). Cells were transformed using the lithium acetate method (Moreno *et al.*, 1991). For temperature-shift experiments, cells were cultured at the permissive temperature of 25°C and shifted to the restrictive temperature of 35.5°C for the indicated times. Media were as described (Moreno *et al.*, 1991). Plasmid pMD71 (carrying *cwg2*) was a gift of Dr A.Duran; *CDC42Sp* borne on pWH5 was a gift of Dr D.I.Johnson; *pck1*, *pck2* and *ppe1* borne on pDB248 were a gift of Dr T.Toda; *kin1* on pDB248 was a gift of Dr D.Levin; and *ras1*, *ral1*, *ral2* and *ral3* on pDB248′ were a gift of Dr M.Yamamoto. We are grateful for all of these gifts.

Mutagenesis was carried out as described (Moreno *et al.*, 1991) using 300 μg/ml *N*-methyl-*N*′-nitro-*N*-nitrosoguanidine for 12 min. The strains used for mutagenesis were *ade6*-M210 *leu1*-32 $h^-$ and *ade6*-M216 *leu1*-32 $h^+$. Cells were plated onto YEA at 25°C for 24 h for recovery, and visually screened using the Singer MSM microscope after a 4 h incubation at 35.5°C. Strains were back-crossed three times prior to genetic analysis. Sterile strains were rescued by genomic *ral1* in pDB248′, allowing them to be crossed.

### *Cytology*

Staining procedures using DAPI were as described (Moreno *et al.*, 1991). Immunofluorescence was performed as described by Hagan and Hyams (1988). Cells were fixed either by mixed aldehyde fixation or in methanol at −20°C for at least 8 min. The primary antibody for microtubule staining was TAT1 (Woods *et al.*, 1989), a kind gift of Dr Keith Gull. The primary antibody for actin staining was a mouse monoclonal no. N350 (Amersham). The secondary antibodies in both cases were Texas Red-linked sheep anti-mouse Ig no. N2031 (Amersham). Cells were examined using a Zeiss Axioskop microscope and photographed on Kodak T-Max 400ASA film.

Time-lapse studies involved placing a thin layer of YEA onto a microscope slide, adding a drop of exponentially growing culture, covering with a coverslip and incubating at the desired temperature inside a sealed Petri dish with damp filter paper to prevent drying of the medium. Measurements of cell dimensions were performed using a drum micrometer attachment.

### *orb5-19 viability studies*

*orb5*-19 was cultured at 25°C and shifted to 35.5°C at time 0. At 2 hourly intervals, samples were withdrawn for determination of cell number by Coulter counting (Moreno *et al.*, 1991). Five hundred cells were plated onto each of two YEA plates and incubated at 25°C until colonies formed. The survival of *orb5*-19 is plotted as a percentage of the number of wild-type colonies at each time point during a parallel experiment.

### *Isolation of orb5 cDNA by complementation of orb5-19*

*orb5*-19 was transformed with an *S.pombe* cDNA library constructed in REP3X (Kelly *et al.*, 1993). Transformants were selected for rescue of lethality on minimal medium supplemented with adenine and were screened visually for rescue of the morphological defect at 35.5°C. Plasmid DNA was recovered from *orb5*-19 clones in which rescue of lethality was linked with the presence of the *LEU2*-based plasmid, and was tested for the ability to rescue *orb5*-19 on retransformation. Three plasmids were isolated, having inserts of 1.5, 1.7 and 2.3 kb. These were shown to encode the same gene by sequencing and Southern analysis.

The 1.5 kb insert was subcloned behind *nmt1* into a vector containing *sup3*-5 and *LEU2*. The construct was transformed into *orb5*-19 *ade6*-704 *leu1*-32 $h^-$ and $ade^+$ transformants selected. Two integrants were crossed to a strain of genotype *leu1*-32 *ade6*-704$h^-$ and analysed by random spore analysis. The *LEU2*, *sup3*-5 and $ts^+$ markers were tightly linked to the *orb5* locus, showing that the insert carries wild-type *orb5*.

Genomic DNA was isolated as described (Moreno *et al.*, 1991). Southern hybridizations using GeneScreen Plus were carried out according to the manufacturer's instructions (DuPont). Probes were prepared from the 1.5 kb orb5 cDNA by random oligo priming with [$^{32}$P]dATP using the Prime-It kit (Stratagene).

Sequencing was carried out using dideoxy chain termination (US Biochemicals). The analysis of the sequence was carried out using the Genetics Computer Group package and comparing with sequences in the SwissProt database.

### *Assay for casein kinase II activity*

Extracts of total protein were prepared from exponentially growing cultures essentially as described (Moreno *et al.*, 1991), but using 20 mM HEPES (pH 7.4) in place of 25 mM MOPS (pH 7.2). Protein concentration was assayed using the BCA (modified Lowry) assay system (Pierce). Kinase activity was measured by incubating 10 μg of protein in a final volume of 15 μl containing 5 mg/ml dephosphorylated casein (Sigma) and 100 μM [$\gamma$-$^{32}$P]ATP (1000–3500 c.p.m./pmol) at 30°C. Reactions were stopped by withdrawing 7.5 μl reaction mixture into 7.5 μl 2 × PAGE sample buffer either immediately after addition of the enzyme or after 10 min of reaction time. Samples were boiled for 3 min prior to electrophoresis. The level of incorporation of radioactive label into each sample was assessed by autoradiography and by scintillation counting of excised gel slices. Final activity was estimated by subtracting the zero time sample from the 10 min sample in each reaction.

## Acknowledgements

We thank A.Duran, M.Yamamoto, T.Toda, D.Levin and D.Johnson for gifts of strains and plasmids, K.Gull for the gift of TAT1, I.Roussou and G.Draetta for communication of unpublished results, and members of the Cell Cycle Group for useful discussions and critical comments on the manuscript, in particular F.Chang, A.Woollard, B.Grallert, F.Verde and K.Hansen. This work was supported by a Wellcome Trust Studentship to V.Snell, and by funding from the Imperial Cancer Research Fund and the Royal Society to P.Nurse.

## References

Chant,J. and Herskowitz,I. (1991) *Cell*, **65**, 1203–1212.
Chant,J. and Pringle,J.R. (1991) *Curr. Opin. Genet. Dev.*, **1**, 342–350.
Chant,J., Corrado,K., Pringle,J.R. and Herskowitz,I. (1991) *Cell*, **65**, 1213–1224.
Chen-Wu,J.L.-P., Padmanabha,R. and Glover,C.V.C. (1988) *Mol. Cell. Biol.*, **8**, 4981–4990.
Diaz,M., Sanchez,Y., Bennett,T., Sun,C.R., Godoy,C., Tamanoi,F., Duran,A. and Perez,P. (1993) *EMBO J.*, **12**, 5245–5254.
Diaz-Nido,J., Serrano,L., Mendez,E. and Avila,J. (1988) *J. Cell Biol.*, **106**, 2057–2065.
Dobrowalska,G., Boldreyff,B. and Issinger,O.-G. (1991) *Biochim. Biophys. Acta*, **1129**, 139–140.
Fawell,E.,Bowden,S. and Armstrong,J. (1992) *Gene*, **114**, 153–154.
Fukui,K. and Kaziro,Y. (1985) *EMBO J.*, **4**, 687–691.
Fukui,K. and Yamamoto,M. (1988) *Mol. Gen. Genet.*, **215**, 26–31.
Fukui,K., Kozasa,T., Kaziro,Y., Takeda,T. and Yamamoto,M. (1986) *Cell*, **44**, 329–336.
Hagan,I.M. and Hyams,J.S. (1988) *J. Cell Sci.*, **89**, 343–357.
Hall,F.L. and Vulliet,P.R. (1991) *Curr. Opin. Cell Biol.*, **3**, 176–184.
Heath,I.B. (1990) *Int. Rev. Cytol.*, **123**, 95–127.
Hiraoka,Y., Toda,T. and Yanagida,M. (1984) *Cell*, **39**, 349–358.
Horio,T., Uzawa,S., Jung,M.K., Oakley,B.R., Tanaka,K. and Yanagida,M. (1991) *J. Cell Sci.*, **99**, 693–700.
Hu,E. and Rubin,C.S. (1990) *J. Biol. Chem.*, **265**, 5072–5080.
Huffaker,T.C., Thomas,J.H. and Botstein,D. (1988) *J. Cell Biol.*, **106**, 1997–2010.
Jacobs,C.W., Adams,A.E.M., Szaniszlo,P.J. and Pringle,J.R. (1988) *J. Cell Biol.*, **107**, 1409–1426.
Johnston,G.C., Prendergast,J.A. and Singer,R.A. (1991) *J. Cell Biol.*, **113**, 539–551.
Kanbe,T., Kobayashi,I. and Tanaka,K. (1989) *J. Cell Sci.*, **94**, 647–656.
Kelly,T.J., Martin,G.S., Forsburg,S.L., Stephen,R.J., Russo,A. and Nurse,P. (1993) *Cell*, **74**, 371–382.
Kikkawa,U., Mann,S.K.O., Firtel,R.A. and Hunter,T. (1992) *Mol. Cell. Biol.*, **12**, 5711–5723.
Kobori,H., Yamada,N., Taki,A. and Osumi,M. (1989) *J. Cell Sci.*, **94**, 635–646.
Levin,D.E and Bishop,J.M. (1990) *Proc. Natl Acad. Sci. USA*, **87**, 8272–8276.
Lozeman,F.L., Litchfield,D.W., Piening,C., Takio,K., Walsh,K.A. and Krebs,E.G. (1990) *Biochemistry*, **29**, 8436–8447.
Madden,K., Costigan,C. and Snyder,M. (1992) *Trends Cell Biol.*, **2**, 22–29.
Maridor,G., Park,W., Krek,W. and Nigg,E. (1991) *J. Biol. Chem.*, **266**, 2362–2368.
Marks,J. and Hyams,J.S. (1985) *Eur. J. Cell Biol.*, **39**, 27–32.
Marks,J., Hagan,I.M. and Hyams,J.S. (1986) *J. Cell Sci. Suppl.*, **5**, 229–241.
Meisner,H., Heller-Harrison,R., Buxton,J. and Czech,M.P. (1989) *Biochemistry*, **28**, 4072–4076.
Miller,P.J. and Johnson,D.I. (1994) *Mol. Cell. Biol.*, **14**, 1075–1083.
Mitchison,J.M. and Nurse,P. (1985) *J. Cell Sci.*, **75**, 357–376.
Moreno,S., Klar,A. and Nurse,P. (1991) *Methods Enzymol.*, **194**, 795–823.
Nadin-Davis,S.A., Nasim,A. and Beach,D. (1986) *EMBO J.*, **5**, 2965–2971.
Nurse,P., Thuriaux,P. and Nasmyth,K. (1976) *Mol. Gen. Genet.*, **146**, 167–178.
Padmanabha,R., Chen-Wu,J.L.-P., Hanna,D.E. and Glover,C.V.C. (1990) *Mol. Cell. Biol.*, **10**, 4089–4099.
Pinna,L.A. (1990) *Biochim. Biophys. Acta*, **1054**, 267–284.
Ribas,J.C., Roncero,C., Rico,H. and Duran,A. (1991a) *FEMS Microbiol. Lett.*, **79**, 263–268.
Ribas,J.C., Diaz,M., Duran,A. and Perez,P. (1991b) *J. Bacteriol.*, **173**, 3456–3462.
Roussou,I. and Draetta,G (1994) *Mol. Cell. Biol.*, **14**, 576–586.
Saxena,A., Padmanabha,R. and Glover,C.V.C. (1987) *Mol. Cell. Biol.*, **7**, 3409–3417.
Serrano,L., Diaz-Nido,J., Wandosell,F. and Avila,J. (1987) *J. Cell Biol.*, **105**, 1731–1739.
Serrano,L., Hernandez,M.A., Diaz-Nido,J. and Avila,J. (1989) *Exp. Cell Res.*, **181**, 263–272.
Shimanuki,M., Kinoshita,N., Ohkura,H., Yoshida,T., Toda,T. and Yanagida,M. (1993) *Mol. Cell. Biol.*, **4**, 303–313.
Streiblova,E. and Wolf,A. (1972) *Z. Allg. Mikrobiol.*, **12**, 673–684.
Strome,S. (1993) *Cell*, **72**, 3–6.
Toda,T., Umesono,K., Hirata,A. and Yanagida,M. (1983) *J. Mol. Biol.*, **168**, 251–270.
Toda,T., Shimanuki,M. and Yanagida,M. (1991) *Genes Dev.*, **5**, 60–73.
Toda,T., Shimanuki,M. and Yanagida,M. (1993) *EMBO J.*, **12**, 1987–1995.
Ulloa,L., Diaz-Nido,J. and Avila,J. (1993) *EMBO J.*, **12**, 1633–1640.
Umesono,K., Hiraoka,Y., Toda,T. and Yanagida,M. (1983a) *Curr. Genet.*, **7**, 123–128.
Umesono,K., Toda,T., Hayashi,S. and Yanagida,M. (1983b) *J. Mol. Biol.*, **168**, 271–284.
Walker,G.M. (1982) *J. Gen. Microbiol.*, **128**, 61–71.
Woods,A., Sherwin,T., Sasse,R., MacRae,T.H., Baines,A.J. and Gull,K. (1989) *J. Cell Sci.*, **93**, 491–500.

*Received on November 25, 1993; revised on December 24, 1993*